A fast calculation algorithm for the charge transfer loss in CCDs

N. Krause[a,*], U.G. Briel[a], M. Popp[a], H. Soltau[b], T. Stadlbauer[a], L. Strüder[a]

[a]*Max-Planck-Institut für Extraterrestrische Physik, Gießenbachstr., D-85740 Garching, Germany*
[b]*KETEK GmbH, Am Isarbach 30, D-85764 Oberschleißheim, Germany*

Abstract

Charge transfer loss due to deep level traps in CCDs is a common phenomenon. In single-photon counting CCDs for X-ray detection, the charge loss results in a degradation of spectroscopic resolution. The transfer loss of a signal depends on various parameters like temperature, number of transferred charges, number of charges in the preceding signals and the elapsed time between these signals. Each signal has to be corrected individually with respect to these parameters. An algorithm based on first principles of capture and emission, that allows a fast determination of the transfer loss is presented. The model was tested on calibration data of an X-ray pn-CCD of the EPIC consortium for XMM. The model describes the experimental data very well.

1. Introduction

At the semiconductor laboratory of the Max-Planck-Institut für Extraterrestrische Physik a pn-CCD for single-photon spectroscopy of X-rays in the soft energy band (100 eV–10 keV) was designed and fabricated for use as a focal instrument of the European Photon Imaging Camera (EPIC) on the XMM (X-ray Multi Mirror) mission of the European Space Agency (ESA). The detector uses pn-junctions instead of conventional MOS-gates and allows full depletion of the detector volume. The transfer channels are read-out parallel. Details of the detector system can be found in Refs. [1,2], its present performance is given in Ref. [3].

Charge transfer loss in the pn-CCD due to deep level traps has been reported previously [4]. The intrinsic impurity and the contamination source are described in more detail in an associated paper [5] also published in this issue. Charge transfer loss is an undesired effect as the signal has to be corrected and the spectral quality declines. The transfer loss due to traps contributes to a spectroscopic loss in two ways: Firstly, the applied correction depends on the signal and operation parameters like the number of generated electrons in the signal (signal charge) and the number of generated electrons of the preceding signals, distance between the signals being transferred, temperature, the transfer length and the clocking scheme. The uncertainties in these parameters result in a broadening of the corrected spectra. Secondly, the transfer loss contributes to the noise [6] due to the statistical behaviour of the capture and emission process.

The goal of this work was to develop a transfer loss model for use in the EPIC pn-CCD calibration and operation that describes the transfer loss quantitatively correct with respect to temperature, signal-charge, precursor signal-charge and the

elapsed time between these signals. From a least-squares fit of the model to pn-CCD calibration data, we determined a set of trap parameters. The model is in very good agreement with the measured charge transfer loss.

Fitting the model to data requires repeated calculation for different sets of parameters. Therefore, the calculation speed of the algorithm is critical. For this reason, we did not use a very successful but slow Monte Carlo simulation of the transfer loss that has been introduced by Meidinger in Ref. [4]. Instead, we have developed an analytical approach which is less time consuming and still precise.

This work is organized as follows: In Section 2, we will derive the charge loss per transfer from first principles of the capture and emission process. The number of trapped charges from previous signals determines the boundary condition for the loss to be calculated. This is determined from a simplified algorithm of the CCD's timing scheme. In Section 3 we present the qualitative behaviour of the model and least-squares fits to EPIC calibration data, in Section 4 the discussion of some limitations and disadvantages of the model is carried out.

2. The charge loss algorithm

2.1. CCD timing scheme and charge transfer

The pn-CCD is a three phase CCD. In the standard imaging mode, charge is collected during the integration time $t_{\mathrm{int}} = 70$ ms and then successively transferred to the On-Chip readout electronics within $t_{\mathrm{readout}} = 4.5$ ms. The transfer mechanism has been described in detail e.g. in Meidingers paper [4]. According to the clocking scheme, each of the 200 pixels of one CCD column must be divided into registers, where the signal charge is stored during transfer for different time intervals. It is appropriate to simplify the charge transfer within one pixel to a storage underneath register $\Phi 1$ for $t_{\Phi 1} \approx 22$ μs and a continuous transfer from $\Phi 1$ to the $\Phi 1$ register of the following pixel within the time $t_{\mathrm{transfer}} \approx 0.7$ μs. The sum of the loss underneath the three registers of a pixel is in the following referred to as loss per pixel transfer.

2.2. Capture and emission of electrons

Impurities with energy levels in the band gap which are located in the transfer area capture and emit electrons of the signal charge. If emission occurs after the charge has been transferred again, the electrons are lost for signal detection. The capture and emission of holes is neglected due to a hole concentration of (ideally) zero in the pn-CCD's bulk. The formulas for the capture probability (per unit time) c_n and emission probability (per unit time) e_n of electrons are explained in detail e.g. in the associated paper [5]. They may be written in the form

$$e_n = AT^2 \exp\left(-\frac{E_{\mathrm{act}}}{KT}\right) \tag{1}$$

$$c_n = \sigma v_{\mathrm{th}} n_{\mathrm{e}} \tag{2}$$

where k is the Boltzmann constant in eV/K, v_{th} the thermal velocity of electrons in cm/s, E_{act} the thermal activation energy for the emission of electrons in eV, n_{e} the free electron density in $1/\mathrm{cm}^3$, A the temperature independent constant in $1/K^2 s$, T the temperature in K, and σ the capture cross-section in cm^2.

2.3. Trap occupation

According to the recombination–generation of charges (see e.g. Ref. [8]) and under the assumption that there are no transitions from and to the valence band, the population–depopulation of traps in the pn-CCD is described by the change in captured electrons due to capture and emission of electrons. We assume that the free electron distribution is in thermal equilibrium and that it depends only on the location within the pixel. After capture or emission, the free electron distribution will redistribute within negligible timescales. As long as the change in the number of free electrons due to trapping is small compared to the number of free electrons, the resulting distribution will be very close to the original one. Furtheron, we assume a uniform distribution of traps. Therefore, the change in captured electrons is given by

$$\frac{\delta n_{\mathrm{ec}}(\boldsymbol{r}, t)}{\delta t} = c_n(\boldsymbol{r}) \cdot (n_{\mathrm{t_o}} - n_{\mathrm{ec}}(\boldsymbol{r}, t)) - e_n \cdot n_{\mathrm{ec}}(\boldsymbol{r}, t). \tag{3}$$

Combined with Eq. (2) this is equal to

$$\frac{\delta n_{\mathrm{ec}}(\boldsymbol{r}, t)}{\delta t} = \sigma v_{\mathrm{th}} n_{\mathrm{e}}(\boldsymbol{r}) \cdot (n_{\mathrm{t_o}} - n_{\mathrm{ec}}(\boldsymbol{r}, t)) - e_n \cdot n_{\mathrm{ec}}(\boldsymbol{r}, t). \tag{4}$$

This is solved by

$$n_{\mathrm{ec}}(\boldsymbol{r}, t) = \frac{n_{\mathrm{t_o}}}{1 + (e_n / c_n(\boldsymbol{r}))} (1 - \exp[-t \cdot (e_n + c_n(\boldsymbol{r}))]) + n_{\mathrm{t}}^0 \exp[-t \cdot (e_n + c_n(\boldsymbol{r}))] \tag{5}$$

where t is the storage time, $n_{\mathrm{e_o}}$ the total density of electrons, $n_{\mathrm{t_o}}$ the total density of traps, n_{t}^0 the total density of occupied traps at $t = 0$, n_{e} the density of free electrons, and n_{ec} the density of captured electrons.

The density of traps $n_{\mathrm{t_o}}$ within the pn-CCD transfer region is at a constant level within the pixel. The density of free electrons varies within the pixel due to the applied potentials and doping. The equilibrium electron distribution has been simulated by the software package TOSCA [7]. As a result, we found that the potential under a collecting register can be approximated with

$$U_{\mathrm{pot}} = \frac{1}{q} (ax^2 + by^2 + cz^2). \tag{6}$$

The parameter a, b and c represent the curvature of the potential in the direction along the three CCD axes, q is the elementary charge. This results in a Gaussian distribution of the free electrons, if we neglect the Coulomb force of the electrons.

$$P(\boldsymbol{r}) \propto \exp\left(-\frac{ax^2 + by^2 + cz^2}{kT} \right) \tag{7}$$

with the condition:

$$\int_V P(\boldsymbol{r}) = N_{\mathrm{e}}. \tag{8}$$

The free electron concentration is then given by the parameters a, b and c and the total number of free electrons N_{e} in the potential minimum of the pixel:

$$n_{\mathrm{e}}(\boldsymbol{r}) = N_{\mathrm{e}} \frac{\sqrt{abc}}{(\pi k T)^{3/2}} \exp\left(-\frac{ax^2 + by^2 + cz^2}{kT} \right). \tag{9}$$

The parameters a, b and c are: $a = 3.1 \times 10^4$ eV cm^{-2}, $b = 4.4 \times 10^5$ eV cm^{-2} and $c = 6.3 \times 10^6$ eV cm^{-2}.

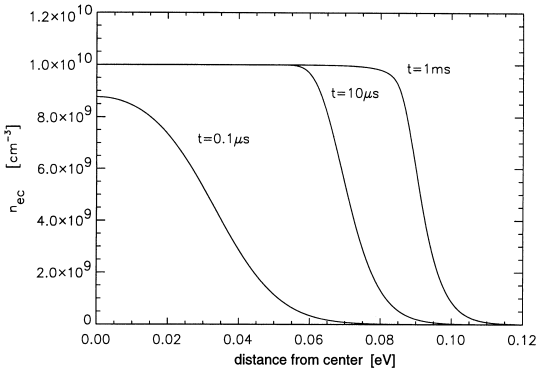

Fig. 1. Calculated density of captured electrons.

To determine the total number of trapped charges N_{ec}, we integrate formula (5). This integration is done numerically.

$$N_{\mathrm{ec}} = \int_V n_{\mathrm{ec}} \, \mathrm{d}V. \tag{10}$$

In Fig. 1, the trap occupation in dependence of the distance from the centre of a register has been calculated for different storage times t. The potential minimum is at the register centre. The trap occupation at $t = 0$ was set to zero, the number of free electrons N_{e} to 1000, the trap parameters to $\sigma = 3 \times 10^{-14}$ cm^2, $n_{\mathrm{t_o}} = 10^{10}$ cm^{-3} and $e_n = 370$ s^{-1}. The temperature was set to 163 K. The parameters have been chosen to match the titanium trap properties as described in Ref. [5]. The electron density at the potential minimum is about three-orders of magnitude higher than the trap concentration. As can be seen from the plot, the number of occupied traps grows with increasing storage time. In the centre of the register, the capture is limited due to trap saturation and at the border due to the concentration-dependent capture rate (Eq. (2)) and the decreasing electron density (Eq. (9)).

2.4. Initial condition

To calculate the charge loss per pixel transfer from the trap parameters σ, $n_{\mathrm{t_o}}$ and e_n, the clocking scheme, the potential parameters a, b and c and the

temperature, one needs to know the distribution of occupied traps in the pixel, before the signal considered is filled into the pixel. This distribution of trapped charge is determined by the "history" of each pixel. Previous signal transfers, emission of captured electrons, scattered light and generation currents result in accumulation of charge in every pixel during the integration time. This establishes a distribution of occupied traps in each pixel.

To take this trap distribution $n_{ec}^0(\boldsymbol{r})$ at $t = 0$ into account, we make the following simplifications:

1. Only one preceding signal charge is considered.
2. The preceding signal is filled into an empty pixel.
3. Trapped charges from the preceding signal are emitted according to $n_{ec}(\boldsymbol{r}, t) = n_{ec}(\boldsymbol{r})^0 \exp(-e_n \cdot \Delta t)$, where Δt is the elapsed time since the preceding signal has been transferred out of that register and n_{ec}^0 is the corresponding trapped electron distribution.
4. Non-signal free charge collected in the $\Phi 1$ registers (assumed to be the same throughout the CCD) during the integration time of the CCD is represented by an equivalent charge called C.
5. The registers except $\Phi 1$ are in repelling state almost all the time. Hence no charge is accumulated underneath these registers. The transfer underneath these registers is split into n-steps with a storage time of $t_{transfer}/n$.

Based on these assumptions, the boundary condition $n_{ec}^0(\boldsymbol{r})$ is determined from the number of electrons in the preceding signal, the elapsed time Δt and the charge C. As the charge C varies with the conditions of the CCD operation, C must be determined from the measurements. Its origin is thermal and light stimulated generation of charge.

2.5. Reemission

Trapped electrons, that are emitted before the signal is transferred not further than one register, drift back into the signal charge due to the drift field between neighbouring registers. This effect reduces the effective trapping for emission times in the order of the transfer time per register. The total number of electrons lost for signal detection is given by the emission probability and the transfer time t_{reg}. In case of the titanium trap, this effect is almost negligible below 190 K.

$$N_{loss} = N_{ec} * [1 - \exp(-e_n t_{reg})] \tag{11}$$

3. Testing the model

In order to test the model, a program has been written that determines the boundary condition and performs the numerical integration of Eq. (10). Results from this code will be discussed and compared with experimental data in the following.

3.1. Qualitative results

Fig. 2 shows the charge loss for different sets of precursor signals (5–100 000 electrons) in dependence of the time difference to the preceding signal transferred Δt for two typical signal charges (500 and 1800 electrons). For the calculation, we used the following parameter set:

$T = 163$ K
$e_n = 370\ s^{-1}$
$\sigma = 3.3 \times 10^{-14}\ cm^2$
$n_{t_0} = 1.7 \times 10^9\ cm^{-3}$
$C = 3$ electrons
$t_{\Phi 1} = 22$ µs, storage time underneath $\Phi 1$
$t_{transfer} = 0.7$ µs, transfer time between $\Phi 1$ registers.

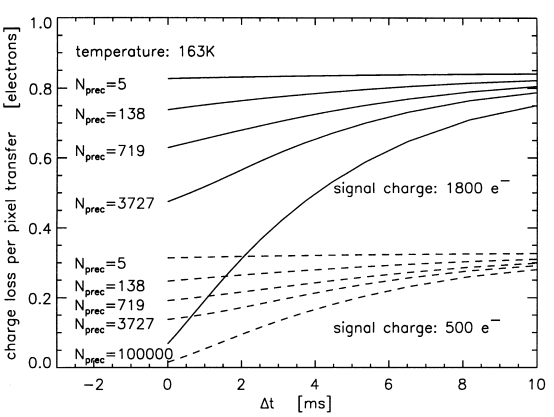

Fig. 2. Dependence of the charge loss per pixel transfer for a set of two signal charges of 1800 and 500 electrons. N_{prec} is the number of electrons in the preceding signal.

The trap-parameters e_n, σ and n_{t_0} again correspond to the pn-CCD's main impurity titanium (see Ref. [5]). For this level, we determined an emission rate of $e_n = 1.3 \times 10^6\ T^2 \exp(-0.258\ \mathrm{eV}/kT)\ \mathrm{K}^{-2}\,\mathrm{s}^{-1}$, which gives $e_n = 370\,\mathrm{s}^{-1}$ at $T = 163$ K. As can be seen from the plot, the model predicts the following behaviour: Decrease of the charge loss due to

- an increase of the preceding signal charge.
- a decrease of the distance in time between two events.

This behaviour is due to the partial saturation of traps from the preceding signal. Generally, preceding signals within $\Delta t \approx 3/e_n$ have to be taken into account. Further, we find a nonlinear dependence of the signal charge itself (see Fig. 4). This behaviour can be explained from the saturation of traps inside a "shell" (compare Fig. 1), where no more electrons can be captured. The shell increases in size with time and the number of free electrons. As a consequence, free charge can be captured only in the outer regions of the shell, where the free electron concentration and hence the capture probability is low. The qualitative results of the model coincides with previous works [4].

3.2. Quantitative results

First tests have been carried out on calibration data of the EPIC pn-CCD camera taken in spring 1998 at the X-ray testing facility PANTER in Munich. The charge loss was extracted from a subset of flat-field (homogeneous intensity of X-rays throughout the CCD) measurements with variations in temperature from 153 to 195 K and signal energies from 278 eV upto 8 keV. The average count rate was approximately 20 counts/s and square centimeter. The X-ray energy is linked to the average number of electrons by the electron–hole creation energy in silicon of about 3.6 eV per electron–hole pair [9]. The charge loss was determined by a linear least-squares fit to selected events in dependence of the transfer length. The slope of the fit gives the (negative) value of the charge loss per pixel transfer.

Fig. 3 shows signal-data in dependence of the transfer length. The events were selected for different distances of the precursor and the precursor energy. The data shown in Fig. 3 were selected to have a precursor with $\Delta t > 3/e_n$, hence $n_{\mathrm{ec}}^0(\boldsymbol{r}) = 0$. The solid line represents the result of a least-squares fit of the data within the dotted lines. The events outside the dotted lines were discarded. For this case, Fig. 4 shows data and a least-squares fit of the model at 163 K for different energies. The data were averaged from 64 channels of the pn-CCD.

Fig. 5 shows the corresponding variation of the parameters capture cross section σ and the equivalent charge C for temperatures from 153 to 195 K.

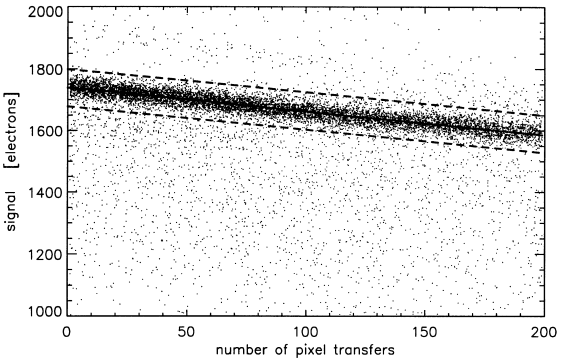

Fig. 3. Signals (dots) in dependence of the transfer length. The signals within the dotted lines were used for analysis. The solid line represents the mean charge loss.

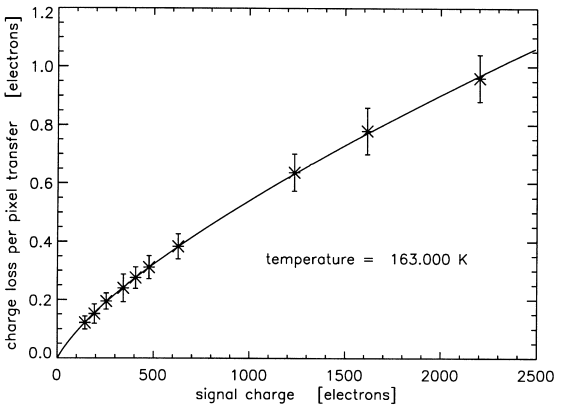

Fig. 4. Dependence of the transfer loss from the signal charge. $\Delta t \geqslant 0.1$ s and $T = 163$ K. This is equivalent with an empty traps condition. The solid line is the resulting charge loss calculated from the model. The employed parameters are based on a least-squares fit of the model to the data (star-shaped symbols with error-bars).

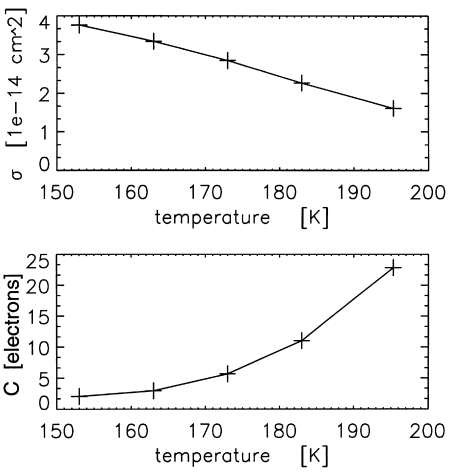

Fig. 5. Variation of the parameters capture cross section and nonsignal free charge C with the temperature as determined from the fit.

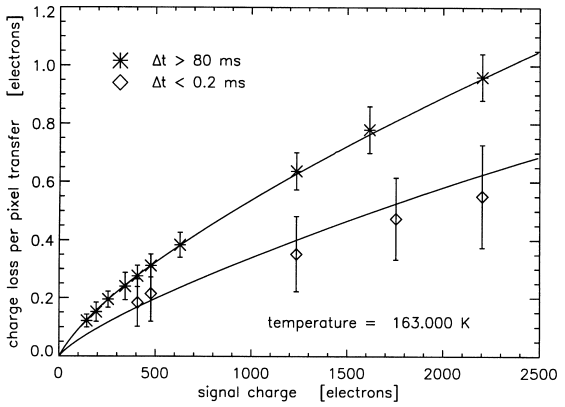

Fig. 6. Dependence of the transfer loss from the signal charge including data with $\Delta t e_n \geqslant 25$ and $\Delta t e_n \leqslant 0.05$. The solid lines represent again the results from the model based on the parameters of a least-squares fit to the data (symbols with error bars).

The concentration was determined from all data to be 1.7×10^9 cm^{-3} and is kept constant for all fits. As can be seen from the figure, the variation of the parameters with the temperature is smooth.

In Fig. 6, the model was fitted to data including signals with precursors within an $\Delta t \leqslant 0.2$ ms (this corresponds to a distance of less than 10 pixels between the two events). The transfer loss decreases due to saturated traps in the pixels. This behaviour is also represented by the model. Due to the low statistics, the errors of the signals with precursors are fairly high. The calculated transfer loss is still well within the error bars of the data. Further test on an enlarged data basis must be done at this point to verify the quantitative correct calculation of the loss in that case.

4. Conclusions

A semi-analytic model for the calculation of charge transfer loss in CCDs was developed. The model describes the qualitative behaviour of the charge transfer loss very well. The quantitative performance could not completely be tested yet, but tests on the energy dependence and on a limited set of preceding signals are very promising. The description of the charge transfer loss for $e_n \Delta t \geqslant 3$ is in excellent agreement with the data. In the pn-CCD operation this is expected to be the most common case that has to be corrected.

There are a number of simplifications in the model and some of them may be changed later in a more sophisticated version. Those are e.g. the number of considered preceding events (now equal one), the change in the electron distribution due to the Coulomb force and the emission and spatial redistribution of charges after the capture. These points may be enhanced on the cost of calculation speed, but for the moment, there is no necessity to do this.

Another more challenging task to be solved is the influence from several sorts of traps. In the pn-CCD, the charge loss is determined by one dominant trap (see Ref. [5]), but there are at least two more traps to be considered in a thorough analysis. Furtheron, additional trap levels are expected to be generated due to radiation damage during the space mission of XMM [10].

Acknowledgements

We wish to thank all (numerous) members of the EPIC calibration team for providing the calibration data, K. Dennerl for his initiative in model improvements and R. Richter for his TOSCA potential simulations.

References

[1] H. Bräuniger et al., Nucl. Instr. and Meth. A 326 (1993) 129.

[2] L. Strüder et al., Nucl. Instr. and Meth. A 288 (1990) 227.

[3] H. Soltau et al., Fabrication and test of a very large X-ray CCD designed for XMM, Nucl. Instr. and Meth. A, 1999, These Proceedings.

[4] N. Meidinger et al., Nucl. Instr. and Meth. A 377 (1996) 298.

[5] N. Krause et al., Metal contamination analysis of the epitaxial starting material for scientific CCDs, Nucl. Instr. and Meth. A, 1999, These Proceedings.

[6] J.D.E. Beynon, D.R. Lamb, Charge-Coupled Devices and Their Applications, McGraw-Hill, New York, 1980, p. 59.

[7] H. Gajewski et al., TOSCA Handbuch, Institut für Angewandte Analysis und Stochastik (IAAS), Karl Weierstraß-Institut, Berlin, 1992.

[8] Landolt-Börnstein, III/22b: Semiconductors: Impurities and Defects in Group IV Elements and III–V compounds, Springer, Berlin, 1989, p. 65.

[9] K. Debertin, R.G. Helmer, Gamma- and X-ray Spectrometry with Semiconductor Detectors, North-Holland, Amsterdam, 1988, p. 74.

[10] N. Meidinger et al., Particle and X-ray damage in pn-CCDs, Nucl. Instr. and Meth. A, 1999, These Proceedings.